

CHARACTERIZATION OF THE ENCAPSULATION PROCESS OF DEEP BRAIN STIMULATION ELECTRODES USING IMPEDANCE SPECTROSCOPY IN A RODENT MODEL

K. Badstübner^{1*}, T. Kröger^{2*}, E. Mix¹, U. Gimsa³, R. Benecke¹ and J. Gimsa^{2**}

¹Department of Neurology, University of Rostock, Gehlsheimer Str. 20, 18147 Rostock, Germany

²Chair of Biophysics, Institute of Biology, University of Rostock, Gertrudenstr. 11A, 18157 Rostock, Germany

³Research Unit Behavioural Physiology, Leibniz Institute for Farm Animal Biology, Wilhelm-Stahl-Allee 2, 18196 Dummerstorf, Germany

* These authors contributed equally to the work.

** Corresponding author.

Keywords: EIS, Intracerebral electrodes, Basal ganglia, Subthalamic nucleus, Rat brain, Chronic instrumentation, 6-OHDA, Parkinson's disease.

Abstract: Deep brain stimulation (DBS) is effective for the treatment of patients with Parkinson's disease (PD), especially in advanced stages which are refractory to conventional therapy. Despite of the regular use in clinical therapy, rodent models for basic research into DBS are not routinely available. The main reason is the geometry difference from rodents to humans, imposing larger problems in the transfer of the stimulation conditions than from primates to humans. For rodents, the development of miniaturized mobile stimulators and stimulation parameters, as well as improved electrode materials and geometry are desirable. The impedance of custom made, cylindrical (contact diameter 200 μm , length 100 μm), platinum/iridium electrodes has been measured *in vivo* for two weeks to characterize the influence of electrochemical processes and of the adherent cell growth at the electrode surface. During the encapsulation process, the real part of the electrode impedance at 10 kHz doubled with respect to its initial value after a characteristic decrease by approximately one third at the second day. An outlook is given on further investigations with different electrode designs for long-term DBS.

1 INTRODUCTION

Parkinson's disease (PD) is a widespread degenerative disorder of the central nervous system that affects motor function, speech, cognition and vegetative functions. The cardinal symptoms such as tremor, rigidity, bradykinesia and postural instability result mainly from the death of dopaminergic cells in the substantia nigra pars compacta and the subsequent lack of dopaminergic inputs into the striatum. This causes an alteration of the activity pattern in the basal ganglia (Braak and Braak, 2000). Deep brain stimulation (DBS) is a novel therapeutic option for PD as well as an increasing number of neuropsychiatric disorders. Before DBS became a therapeutic intervention, electric stimulation of basal ganglia had been used to guide neurosurgeons to the

precise position for a surgical lesion, the ultimate therapy of a late-stage PD. The main advantage of DBS over surgical lesions is the reversibility and possibility to modulate stimulation parameters (Benabid et al., 1987). The small volume of the target region for DBS in the human brain requires a highly specific adaption of the electrodes which need to be thoroughly tested in animal models, including different materials and geometries. So far, DBS data of animal models of PD are scarce. During *in vivo* stimulation, the properties of the DBS electrodes are changing as a function of time caused by electrochemical processes at the surface of the implant and the subsequent tissue response (Gimsa et al., 2005). The tissue response is a foreign substance reaction. Its intensity depends on the material (Grill and Mortimer, 1994) and is correlated with the thickness of the adventitia finally

encapsulating the implant (Wintermantel et al., 2002). Adventitia formation causes a steady change in the impedance of the electrodes leading to changes in the attenuation of the stimulating signal. As a result, the efficiency of the surrounding tissue stimulation is changing (Lempka et al., 2009 and 2011; Grill and Mortimer, 1994). One opportunity to minimize this problem is to choose an appropriate electrode material. Previous investigations of our group (Gimsa et al. 2006; Henning et al., 2007) have shown that the use of stainless steel electrodes is not appropriate because of the corrosion and erosion processes intensified by electrolytic electrode processes. Electrochemically induced alterations are negligible for inert platinum electrodes, even though electrode processes may still influence the surrounding tissue (Gimsa et al., 2005). For an optimal adjustment of the DBS signal, the kinetics of the electrode impedance alterations caused by the adventitia formation must be taken into account (Lempka et al., 2009 and 2011).

2 MATERIALS AND METHODS

2.1 Animal Treatment

A number of 30, adult, male Wistar Han rats (240-260 g) were obtained from Charles River Laboratory, Sulzfeld, Germany) and housed under temperature-controlled conditions in a 12 h light-dark cycle with conventional rodent chow and water provided *ad libitum*. The rats were subject to the following treatments:

- anesthesia
- 6-OHDA-lesioning (28 rats)
- electrode implantation (6 rats)
- impedance measurement (2 rats)

The study was carried out in accordance with European Community Council directive 86/609/EEC for the care of laboratory animals and was approved by Rostock's Animal Care Committee (LALLF M-V/TSD/7221.3-1.2-043/06).

2.1.1 Anesthesia

The rats were anesthetized by ketamine-hydrochloride (10 mg per 100 g body weight, i.p., Ketanest S[®], Pfizer, Karlsruhe, Germany) and xylazine (0,5 mg per 100 g body weight, i.p., Rompun[®], Pfizer). Before surgery, the eyes of the rats were medicated with Vidisic (Bausch and Lomb, Berlin Germany). After surgery, the wound was sutured and the rats received 0.1 ml

novaminsulfone (Ratiopharm, Ulm, Germany) and 4 ml saline subcutaneously. Rats were exposed to red light (Petra, Burgau, Germany) until normalization of vital functions.

2.1.2 6-Hydroxydopamine (6-OHDA) Lesioning

The 6-OHDA (Sigma, Deisenhofen, Germany) lesioning was performed by stereotactic surgery in adaption to Kirik et al. (1998). The lesions of the right medial forebrain bundle of rats were made by injection of 26 µg 6-OHDA in 4 µl saline with 1 g/l ascorbic acid delivered over 4 min via a 5 µl hamilton microsyringe (Postnova Analytics, Landsberg/Lech, Germany). The coordinates relative to bregma were: anterior-posterior (AP) = -2.3 mm, medial-lateral (ML) = 1.5 mm and dorsal-ventral (DV) = -8.5 mm (Paxinos and Watson, 1998).

2.1.3 Electrode Implantation

Electrodes were implanted into the subthalamic nucleus (STN), which is the most common target region for treatment of PD patients. The surgical procedure was performed using a stereotactic frame (Stoelting, Wood Dale, IL, USA) modified according to Harnack et al. (2004). To support the surgical procedure, a cold light source (KL 1500 LCD, Schott, Mainz, Germany) was used in combination with a stereo-microscope (Leica, Wetzlar, Germany). The skull was opened by a dental rose-head bur (Kaniedenta, Germany). The coordinates relative to bregma were: anterior-posterior (AP) = -3.5 mm, medial-lateral (ML) = 2.4 mm and dorsal-ventral (DV) = -7.6 mm (Paxinos and Watson, 1998). A dental drill was used to bore an additional hole in the skull for an anchor screw. The electrode was fixed to the skull by an adhesive-glue bridge (Technovit 5071, Heraeus, Germany) to the anchor screw.

Counter-electrode wires were implanted into the neck of the rats.

2.2 Stimulation- and Counter-electrodes

For impedance measurements, we designed unipolar platinum-iridium (Pt/Ir) microelectrodes which were covered with polyesterimide insulation and custom-made by Polyfil (Zug, Switzerland; Figure 1).

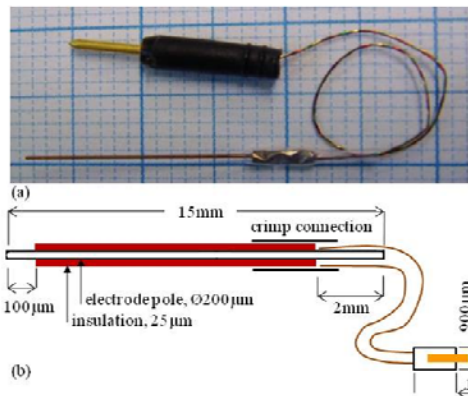


Figure 1: Photograph (a) and scheme (b) of the unipolar Pt/Ir electrode. The electrode pole was a round wire made from Pt90Ir10 with a diameter of 200 μm . The length of the non-insulated tip of the electrode pole was 100 μm . The insulation consisted of polyesterimide 180 with a thickness of 25 μm (Nowak et al., 2011).

Dental wires made of biocompatible, nickelfree steel alloy (18% Cr, 18% Mn, 2% Mo, 1% N, remainder iron) of 1 mm diameter and 10 mm length were used as counter electrodes (see: Figure 4) in combination with the unipolar DBS electrodes (Figure 1).

Electrochemical electrode effects were negligible at the counter electrode due to the low current density at its large surface.

2.3 Electric Impedance Spectroscopy (EIS)

Electric impedance spectroscopy (EIS) is a common measuring technique for determining the electrical properties of tissues (Foster and Schwan, 1989). It is used in a wide range of applications, such as breast cancer detection (Kerner et al., 2002), the monitoring of the lung volume (Adler et al., 1997) and in material sciences. EIS is nondestructive and therefore suitable for the characterization of the DBS electrodes during the encapsulation process.

Equipment

The EIS measurements were conducted with an impedance spectrometer Sciospec ISX3 (Sciospec Scientific Instruments, Pausitz, Germany) and a test fixture HP16047D (Hewlett-Packard, Japan) connected to a personal computer with Sciospec-measuring software. The two connectors of the test fixture were connected to the DBS and the counter electrodes.

Measurement

To characterize the electrode properties during encapsulation, the impedance was recorded in the frequency range from 100 Hz to 10 MHz over a

period of two weeks after implantation. Frequency range, amplitude, number of points and the averaging of the impedance spectrometer were programmed by the measuring-software (Sciospec). 401 frequency points were logged which were distributed equidistantly over a logarithmic frequency scale. The measuring voltage (peak to peak) was 12.5 mV_{pp}. The measuring-software logged the measuring data of the impedance spectrometer (real and imaginary parts of the impedance vs. frequency), saving them to a file.

Before each measurement, the impedance spectrometer was calibrated by open, short and load measurements. Each measurement was repeated three times to improve the statistical significance. The measurements were repeated every day for one week and every second day during the second week.

The stimulation pulse usually applied in DBS has a frequency of 130 Hz and a pulse width of 60 μs . Because of the steep slopes of the needle-shaped pulse, the signal is rich in high harmonic frequencies (Gimsa et al. 2005). For this reason, we measured the impedance within the wide frequency range from 100 Hz to 10 MHz, which is beyond the range of up to 10 kHz reported by Lempka et al. (2009).

Impedance theory

The electrical impedance describes the magnitude ratio between the applied AC voltage and the resulting current flowing with a certain phase shift. Mathematically speaking, the impedance Z^* is a complex number with the unit [Ω], which is composed of a real (Z') and an orthogonal imaginary part (Z'') marked by the complex unit $j = \sqrt{-1}$:

$$Z^* = \text{Re}(Z^*) + j \cdot \text{Im}(Z^*) = Z' + j Z'' \quad (1)$$

For interpretation of the measuring data, an equivalent circuit model is required to be fitted to the measuring data. The aim was to model electrochemical processes and adherent cell growths by combinations of resistors, capacitors and constant phase elements (Lempka et al., 2009).

Data analysis

The logged data were transferred to Matlab (The MathWorks™, Version 7.9.0.529) to calculate means and standard deviations. For their graphic representation, they were finally copied to Sigma Plot 11.0 (Systat Software, 11.0, Build 11.2.0.5).

2.4 Electron Microscopy Study of Electrode Encapsulation by Tissue

Concentric bipolar microelectrodes with an inner

pole diameter of 75 μm and an outer pole diameter of 250 μm (CB CSG75; FHC, Bowdoinham, ME) were placed into the STN of two anesthetized rats. The rats were stimulated for 3 h with biphasic constant-current pulses with a repetition frequency of 130 Hz and pulse duration of 60 μs at 250 μA with a stimulus generator (Multichannel Systems, Reutlingen, Germany). The electrodes were removed and one electrode was incubated in trypsin solution (Trypsin-EDTA (1x) in HBSS W/O CA&MG W/EDTA.4NA, Gibco, UK) at 37°C for 1 h. The other electrode was postfixed overnight in 4% glutaraldehyde (Merck, Germany) in PBS.

Electrodes were washed, fixed in 4% glutaraldehyde in PBS, washed again, postfixed in 1% osmium tetroxide, dehydrated in acetone, and subjected to critical-point drying (EMITECH K850, Ashford, Kent, UK). The samples were sputtered with colloidal gold using a Sputter Coater (BAL-TEC SCD 004, Schalksmühle, Germany) before examination in the SEM (DSM 960 A, Zeiss, Oberkochen, Germany).

3 RESULTS

3.1 Stimulation- and Counter Electrode Implantation

As a first test, the localization of the electrode tip in the target region was verified by ink injection via a 5 μl hamilton microsyringe of approximately the same size as the implanted stimulation electrode (Figure 2).

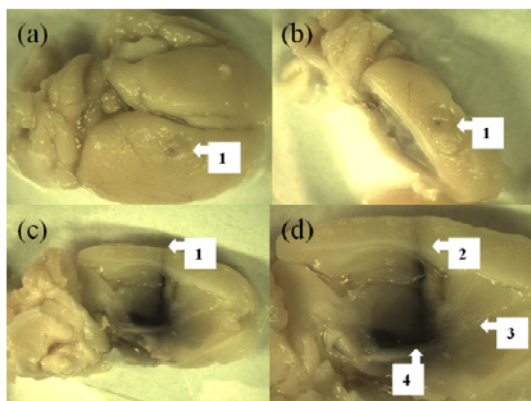


Figure 2: Rat brain fixed in formalin, (a): top view of a rat brain with a puncture resembling an electrode canal (1), (b): sagittal section of one hemisphere with the puncture (1), (c): hemisphere with tissue removed to the injection canal, (d): enlarged photo of (c) with ink injection canal (2), striatum (3), and basal ganglia (4).

Chronic instrumentation was established and applied to freely moving PD -rats (Figure 3). For this, a commercial rat jacket (Lomir Biomedical, Quebec, Canada) with a backpack was used. All electronic components (Figure 2) were located in the backpack. This allowed for a stimulation of up to six weeks when the batteries were changed every second day.

For the EIS measurements, counter electrodes were pierced through the intact scalp close behind the cut for the implantation of the stimulation electrode. An example of implantation of a counter electrode using dental wire of biocompatible steel alloy is shown in Figure 4.

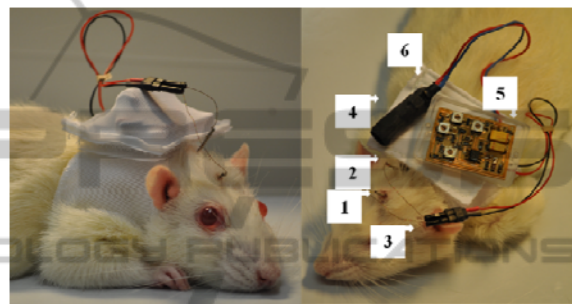


Figure 3: Photograph of a rat that was anesthetized for implantation of chronic instrumentation consisting of: (1): Pt/Ir electrode, (2): counter-electrode, (3): plug-connector electrodes, (4): battery, (5): DBS-stimulator and (6): carrying bag.

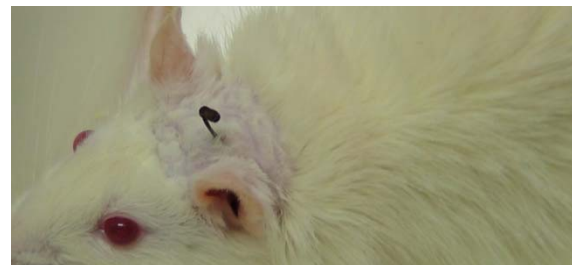


Figure 4: Implanted dental wire of biocompatible steel alloy used as counter electrode for the EIS measurement.

3.2 Impedance Measurement

Our data showed the general tendency of an impedance increase during the encapsulation process. The measuring results are shown in Figure 6. After 12 days, the value of Z' (Figure 6a) has almost doubled compared to its initial value at 10 kHz. In parallel, also the absolute value of Z'' (Figure 6b) increased. The results match with findings of Lempka et al. (2009) for the monkey brain. The main reason for the impedance increase is the formation of the adventitia as a foreign substance

reaction. Indeed, the adventitia covered the electrode surface as shown by Lempka et al. (2009). Our own electron-microscopy study showed that stimulation electrodes get overgrown by cells within 3h post implantation (Figure 5).

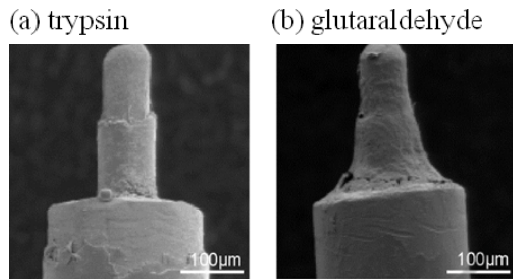


Figure 5: Scanning electron-microscopical images of electrodes that had been implanted and used for 3 h of stimulation. (a): Electrode cleaned by trypsin prior to electron microscopy. (b): Electrode fixed with adhering tissue.

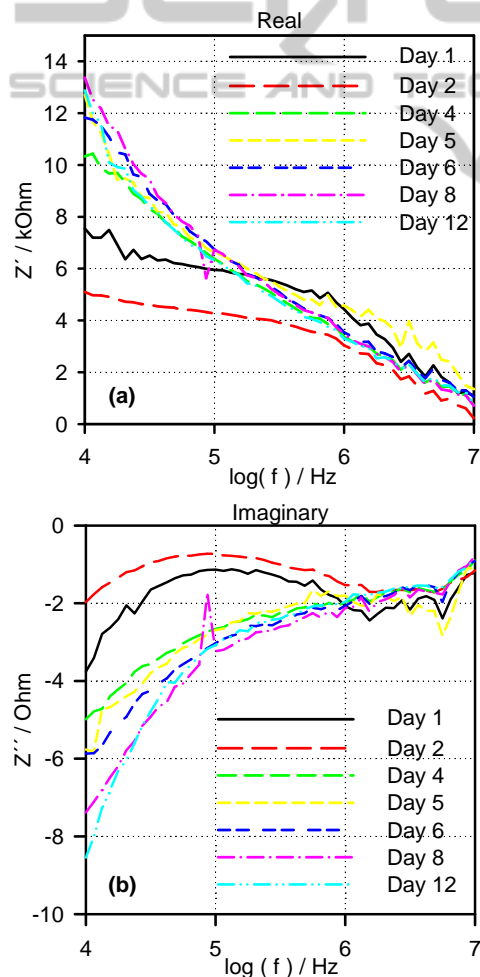


Figure 6: *In vivo* impedance measurements with a unipolar Pt/Ir electrode in combination with a steel alloy counter-electrode ((a) Z' ; (b) Z'').

Our data showed an impedance decrease at the second day after implantation followed by a significant increase from the third day onwards. Interestingly, the same impedance behavior has already been reported by Lempka et al. (2009, p. 6, Figure 4). However, no explanation has been given for this phenomenon.

4 CONCLUSIONS AND PERSPECTIVES

Pilot experiments in the rat model have shown that the impedance of a unipolar DBS electrode is significantly increasing with time after implantation. In future experiments, different biocompatible electrode materials such as titanium, diverse titanium alloys, platinum, gold, silver and stainless steel will be tested. For these tests, an array of various counter electrodes will be pierced into the necks of a number of rats.

In addition, bipolar electrodes possessing modified configurations such as shifted tips will be used to test the effects of non-axial symmetric field distributions.

The equivalent circuit model will be improved for a better understanding of the measuring data in order to extract encapsulation parameters. These investigations aim at clarifying the phenomenon of the impedance drop at the second day after implantation.

Potential effects at the electrode-tissue-interface will be analyzed by histological, immunochemical and electron-microscopical methods.

ACKNOWLEDGEMENTS

K.B. is grateful for a stipend of the German Research Foundation (DFG, Research Training Group 1505/1 “welisa”). T.K. acknowledges financing by a project of the Federal Ministry of Economics and Technology (BMW, V230-630-08-TVMV-S-031). Part of the work was conducted within a project financed by the Federal Ministry of Education and Research (BMBF, FKZ 01EZ0911). The authors are grateful to Dr. J. Henning for help with the electron microscopy study and would like to thank the staff of the electron microscopy center at the University of Rostock's Medical Faculty for outstanding technical support.

REFERENCES

- Adler, A., Amyot, R., Guardo, R., Bates, J. H., Berthiaume, Y., 1997. Monitoring changes in lung air and liquid volumes with electrical impedance tomography. *Journal of Applied Physiology*. 83(5): 1762-7.
- Braak, H., Braak, E., 2000. Pathoanatomy of Parkinson's disease. *Journal of Neurology*. 247(2): II3-10.
- Benabid, A. L., Pollak, P., Louveau, A., Henry, S., de Rougemont, J., 1987. Combined (thalamotomy and stimulation) stereotactic surgery of the VIM thalamic nucleus for bilateral Parkinson disease. *Applied Neurophysiology*. 50(1-6): 344-6.
- Foster, K. R., Schwan, H. P., 1989. Dielectric properties of tissues and biological materials: a critical review. *Critical reviews in biomedical engineering*. 17(1): 25-104.
- Gimsa, J., Habel, B., Schreiber, U., van Rienen, U., Strauss, U., Gimsa, U., 2005. Choosing electrodes for deep brain stimulation experiments – electrochemical considerations. *Journal of Neuroscience Methods*. 142(2): 251-65.
- Gimsa, U., Schreiber, U., Habel, B., Flehr, J., van Rienen, U., Gimsa, J., 2006. Matching geometry and simulation parameters of electrodes for deep brain stimulation experiments – numerical considerations. *Journal of Neuroscience Methods*. 150(2): 212-27.
- Grill, W. M., Mortimer, J.T., 1994. Electrical properties of implant encapsulation tissue. *Annals of Biomedical Engineering*. 22(1): 23-33.
- Henning, J., 2007. Wirkungen der tiefen Hirnstimulation – Analyse der Gen- und Proteinexpression in einem optimierten Rattenmodell. *Dissertation*. University of Rostock.
- Harnack, D., Winter, C., Meissner, W., Reum, T., Kupsch, A., Morgenstern, R., 2004. The effects of electrode material, charge density and stimulation duration on the safety of high-frequency stimulation of the subthalamic nucleus in rats. *Journal of Neuroscience Methods*. 138(1-2): 207-16.
- Kerner, T. E., Paulson, K. D., Hartov, A., Soho, S. K., Poplack, S. P., 2002. Electrical impedance spectroscopy of the breast: clinical imaging results in 26 subjects. *IEEE Transactions on medical imaging*. 21(6): 638-45.
- Kirik, D., Rosenblad, C., Björklund, A., 1998. Characterization of behavioral and neurodegenerative changes following partial lesions of the nigrostriatal dopamine system induced by intrastriatal 6-hydroxydopamine in the rat. *Experimental Neurology*. 152(2): 259-77.
- Lempka, S. F., Miocinovic, S., Johnson, M. D., Vitek, J. L., McIntyre, C. C., 2009. In vivo impedance spectroscopy of deep brain stimulation electrodes. *Journal of Neural Engineering*. 6, 046001, 11pp.
- Lempka, S. F., Johnson, M. D., Moffitt, M. A., Otto, K. J., Kipke, D. R., McIntyre, C. C., 2011. Theoretical analysis of intracortical microelectrode recordings. *Journal of Neural Engineering*. 8(4):045006.
- Macdonald, J. R., 1992. Impedance spectroscopy. *Annals of Biomedical Engineering*. 20(3): 289-305.
- Nowak, K., Mix, E., Gimsa, J., Strauss, U., Sriperumbudur, K. K., Benecke, R., Gimsa, U., 2011. Optimizing a rodent model of Parkinson's disease for exploring the effects and mechanisms of deep brain stimulation. *Parkinson's Disease*. 2011: 414682.
- Wintermantel, E., Ha, S-W., 2002. *Medizintechnik mit biokompatiblen Werkstoffen und Verfahren*. Springer, Berlin, 3rd edition: 134-5.
- Paxinos, G., Watson, C., *The rat brain in stereotaxic coordinates*. Academic Press, San Diego, 1998.